NANO LETTERS

Letter

pubs.acs.org/NanoLett

Programmable Quantitative DNA Nanothermometers

David Gareau,[†] Arnaud Desrosiers,[†,‡] and Alexis Vallée-Bélisle*[,†,‡]

[†]Laboratory of Biosensors and Nanomachines, Département de Chimie and [‡]Département de Biochimie et Médecine Moléculaire, Université de Montréal, C.P. 6128, Succursale Centre-ville, Montréal, Québec H3C 3J7, Canada

Supporting Information

ABSTRACT: Developing molecules, switches, probes or nanomaterials that are able to respond to specific temperature changes should prove of utility for several applications in nanotechnology. Here, we describe bioinspired strategies to design DNA thermoswitches with programmable linear response ranges that can provide either a precise ultrasensitive response over a desired, small temperature interval (±0.05 °C) or an extended linear response over a wide temperature range (e.g., from 25 to 90 °C). Using structural modifications or inexpensive DNA stabilizers, we show that we can tune the transition midpoints of DNA thermometers from 30 to 85 °C. Using multimeric switch architectures, we are able to create ultrasensitive thermometers that display large quantitative fluorescence gains within small temperature variation (e.g., > 700% over 10 °C). Using a combination of thermoswitches of different stabilities or a mix of stabilizers of various strengths, we can create extended thermometers that respond linearly up to 50 °C in temperature range. Here, we demonstrate the reversibility, robustness, and efficiency of these programmable DNA thermometers by monitoring temperature change inside individual wells during polymerase chain reactions. We discuss the potential applications of these programmable DNA thermoswitches in various nanotechnology fields including cell imaging, nanofluidics, nanomedecine, nanoelectronics, nanomaterial, and synthetic biology.

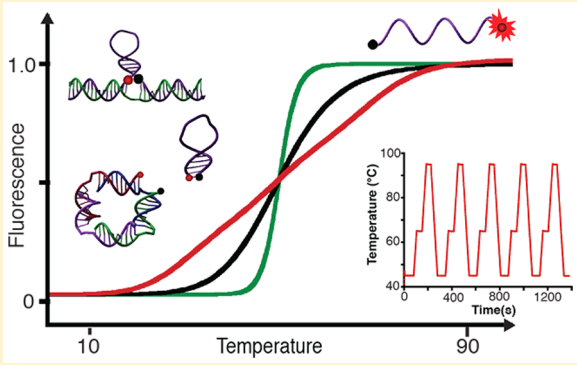

KEYWORDS: *Nanothermometry, molecular switches, DNA nanotechnology, biosensors, PCR, fluorescence*

Temperature is a key parameter, which controls the dynamic of all chemical, physical, and biological systems. With the advance of nanotechnology, it becomes imperative to develop tools that can precisely measure local temperature at the nanoscale. Such nanothermometers would prove useful in fields such as nanoelectronic,[1] nanophotonics,[2] microfluidics,[3] and nanomedecine.[4] A handful of thermoresponsive nanothermometers have been developed over the past decade. These include quantum dot nanocrystals,[5] nanoparticle-based systems,[6−8] nanogels,[9,10] nanodiamonds,[11] polymers,[12,13] and proteins,[14] and DNA-based thermometers.[15−17] These nanothermometers were applied to measure, for example, temperature variations in microfluidic devices[8] and inside living cells.[11,13] Despite these recent advances in nanothermometry, however, many drawbacks still limit the practicability and thus the usefulness of these approaches. These limitations include poor biocompatibility, low-temperature resolution, slow response time, complex synthesis, expensive instrumentation, low level of programmability, and complex nonlinear responses.[18,19]

Among the various nanothermometers described above, those working via a structure-switching mechanism[12−17] represent a promising avenue. This is because these thermoswitches can potentially be adapted to provide different signal readouts[20] and can serve as building blocks to engineer more advanced thermoresponsive materials for applications such as drug delivery.[21] Most specifically, switch-based nucleic acid thermometers,[15−17] display a high potential for nanothermometry, as exemplified in living organisms, which employ finely thermoregulated RNA switches to modulate and tune a number of biological activities such as gene expression.[22] Lately, several groups (e.g., Yang,[15] Andersen,[16] and Kompany-Zareh[17]) have thus proposed to use simple DNA stem-loops (similar to molecular beacons[23]) as fluorescent nanothermometers. These DNA stem-loops work by exploiting the well-known melting transition of their double helix stem that can unfold at specific temperatures determined by the stem stability (Figure 1a). When a fluorophore (6-FAM) and a quencher (BHQ- 1) are attached at both extremities of this stem-loop (Figure 1a), the fluorophore-quencher pair separates upon switch unfolding giving rise to a typical 5-fold linear increase in fluorescence over a 12−15 °C interval (Figure S1). Despite the promising features of these stem-loop thermometers, which include fast response times and sustained efficiency over several cycles,[15] a main drawback affects their performance: their linear ranges remain fixed over 12−15 °C. This fixed dynamic range creates three main complications. First, a new stem-loop must be synthesized for each new specific application thus rendering this approach expensive and labor-intensive (a typical dual-labeled DNA ranges from $250−400).

Received: January 13, 2016
Revised: April 4, 2016
Published: April 8, 2016

DOI: 10.1021/acs.nanolett.6b00156
Nano Lett. 2016, 16, 3976−3981

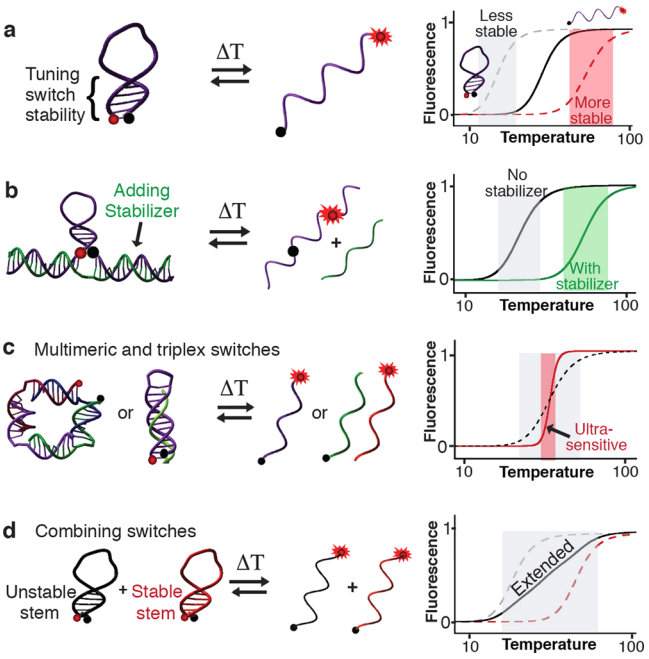

Figure 1. Bioinspired strategies to engineer programmable DNA-based nanothermometers. (a) Tuning the dynamic range of the nanothermometer by modifying the stability of the switch. (b) Tuning the dynamic range of the nanothermometer by adding an inexpensive, unlabeled allosteric DNA stabilizer strand. (c) Enhancing the signal gain (sensitivity) of the nanothermometer by engineering multimeric switch architectures. (d) Extending the dynamic range of the nanothermometer by combining switches (or stabilizers) with different stabilities.

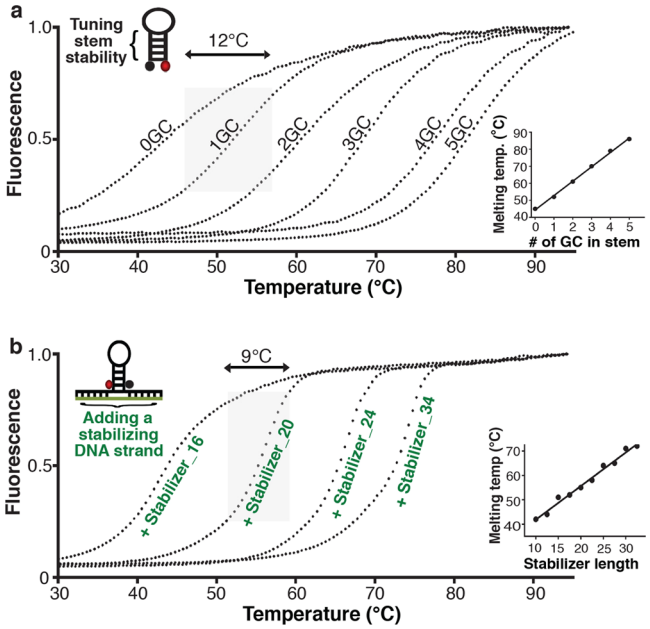

Figure 2. Tuning the dynamic range of DNA nanothermometers by varying the GC content in the stem or by adding DNA stabilizers. (a) Tuning the dynamic range of DNA nanothermometer by varying the AT and GC content in stem. Inset: stem-loop melting temperature in function of the number of GC in the stem. (b) Tuning the dynamic range of a nanothermometer by adding inexpensive, unlabeled DNA stabilizers of various lengths. The stabilizer stabilizes the DNA stem by hybridizing to DNA overhangs at the extremity of the switch (for clarity, only four stabilizers are shown in the figure). Of note, these bimolecular thermoswiches display a more cooperative melting transition than the unimolecular stem-loop (9 °C versus 12 °C). Inset: stem-loop melting temperature in function of the length of the stabilizer. All experiments were conducted using 25 nM of switches and 100 nM of stabilizers in 50 mM $NaPO_4$ with 100 mM NaCl at pH 7.0.

Second, stem-loop thermometers only produce weak signal gains when measuring small temperature variations (e.g., 80[15] and 35%,[16] fluorescence gain over a 10 °C interval). This weak sensitivity precludes precise temperature sensing when only small temperature changes take place (e.g., ±1 °C). Third, the fixed 12−15 °C dynamic range limits the capacity of stem-loop thermometers to measure temperature variations spanning more than 15 °C. In response to these limitations, we describe here various bioinspired strategies to engineer DNA thermoswitches with programmable sensitivities and dynamic ranges (Figure 1).

In order to shift the dynamic range of a DNA stem-loop so that it responds to different specific temperature variations, Jonstrup et al. have proposed to modulate the stem stability by changing either the buffer ionic strength (Figure S1) or the GC content of the stem (Figure 2a).[16] By varying salt concentration (NaCl), we can tune the melting temperature (and thus the dynamic range) of the stem-loop switch by up to 30 °C (Figure S1). However, changing the ionic strength may not be an option for tuning stem stabilities in applications such as in vivo temperature monitoring. Alternatively, DNA stem stability can also be modulated by substituting one AT base pair to a more stable GC base pair. For example, the melting transition of a 5-base pair stem-loop thermoswitch can be increased by roughly 10 °C per AT to GC substitutions, going from 45 to 90 °C (Figure 2a).

The main limitation of current DNA thermometers, however, is their inability to be tuned to respond to different temperature ranges. To overcome this, we propose here to employ a bioinspired allosteric regulation mechanism and re-engineer the DNA stem-loop so that it can be programmed to respond to many desired temperature windows via the addition of a simple, inexpensive DNA stabilizer (Figures 1b and 2b).[24] For a DNA stem-loop switch, this is easily achieved by adding overhang DNA sequences at both extremities of the stem. A stabilizer can then be easily designed to bind these overhangs, which will stabilize the stem and shift the melting transition of the switch to higher temperatures (Figure 2b). Using DNA stabilizers of various lengths, we can tune the melting temperature and dynamic range of a single stem-loop switch by up to 30 °C (~3.6 °C on average per additional base on each side of the stabilizer) (Figure 2b inset). Another advantage of this stabilizer strategy is that it enables to tune "on-the-fly" the stability of a DNA stem-loops thermometer, and therefore its dynamic range, via the addition of a simple, inexpensive DNA strands to your experimental setup.

One promising feature of DNA-based thermometers is their fast response time, which is linked to the folding/unfolding rates of the DNA structures. In order to characterize the temporal resolution of the unimolecular (Figure 2a) and bimolecular (Figure 2b) stem-loops, we determined the folding/unfolding rates of these structures (Figure S2). Using rapid [NaCl]-jump experiments, we show that the unimolecular stem-loop folds and unfolds faster than the dead time of our mixing instrument (3.2 ms) as this has been previously observed for other similar DNA stem-loops.[25] Although being significantly slower that its unimolecular counterpart, the bimolecular tunable stem-loop still provides a relatively rapid

DOI: 10.1021/acs.nanolett.6b00156
Nano Lett. 2016, 16, 3976−3981

response time within a few seconds ($t_{1/2} \approx 0.08$ and 2 s for unfolding and folding, respectively at 45 °C) (Figure S2).

For some applications, the 12−15 °C unfolding dynamic range of the unimolecular stem-loop thermoswitch is too broad, thus limiting the ability to achieve sufficiently high signal gain when measuring small temperature changes. For example, stem-loop thermometers explored by Yang,[15] Andersen,[16] and Kompany-Zareh[17] produce only 80, 35, and 250% fluorescence gain, over a 10 °C interval, respectively. This weak sensitivity reduces their usefulness in applications where only small temperature changes take place (±1 °C) (e.g. in vivo imaging applications[17]). In order to develop DNA switches with higher signal gain, we explored the unfolding transition of alternative more complex DNA folds, such as the DNA triplex helix, and the DNA G-quadruplex structure,[26−28] hoping that they may display more cooperative melting transition (Figure S3). We found that both these DNA folds display a convenient single unfolding transition albeit with a sharper (triplex, 10 °C) and a more extended dynamic range (G-quadruplex, from 40 to 60 °C).

Inspired by the more cooperative melting behavior of the DNA triplex fold (Figure S3) and by the convenient properties of the tunable "allosteric" stem-loop (Figure 2b), we decided to combine both features into a single design in order to create an ultrasensitive, tunable, DNA thermometer. To do so, we exploited a DNA-clamp architecture[29] in which a polypurine DNA strand is stabilized in a clamp conformation following its hybridization to a second polypyrimidine DNA strand via the formation of Watson−Crick and Hoogsteen interactions (see Material and Methods and ref 29). We find that the melting transition of this tunable DNA triplex clamp displays a much more cooperative transition (e.g., 3-fold larger fluorescence variation between 35 and 40 °C) with a linear dynamic range spanning less than 7 °C (Figure 3a, green dotted line). Notably, the triplex clamp switch also displays a lower background fluorescence (<10%) at low temperature thus enabling an unprecedented high signal gain over small temperature windows. For example, a comparable stem-loop thermometer (0GC) typically displays a 135% gain of fluorescence within the 30−40 °C interval (Figure 3a, black dotted line) while the tunable clamp switch displays a 710% gain of fluorescence in the same interval. This enables the DNA-clamp switch to detect temperature changes as small as 0.05 °C (Figure 3b and see Material and Methods for the determination of this precision). In addition, we find that the melting transition of this DNA clamp switch can be finely tuned from a 30 °C melting midpoint to an arbitrarily higher temperature through 2 °C increments by simply adding extra triplex-forming nucleotides in the stabilizer (Figure 3a, right inset). This highly sensitive DNA clamp switch, albeit with a limited dynamic range (7 °C), therefore represents an ideal nanothermometer to measure small temperature changes near biologically relevant temperatures (Figure 3b, right inset).

Encouraged by the ability of bimolecular switches (and other highly complex DNA structures) to provide steeper melting transitions (see also ref 28), we further explored the ability of multimeric DNA switches to display higher cooperative melting behavior (Figure 1c). We tested this idea by engineering a trimeric "triangle-like" DNA structure as well as a tetrameric "square-like" DNA structure (Figure S4). As expected, both these multimeric switches display a steeper melting transition compared to the unimolecular stem-loop thermoswitch with a dynamic range spanning only 7 °C (triangle) and 8 °C (square). Similarly to the triplex clamp switch, they also enable

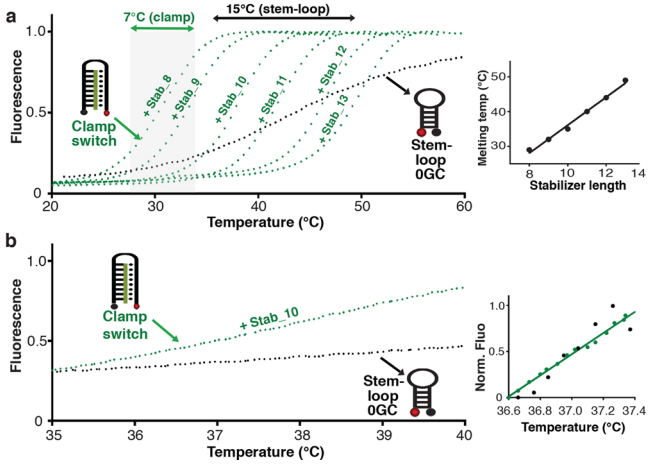

Figure 3. A high gain, ultrasensitive, tunable DNA clamp thermoswitch. (a) The highly cooperative melting transition of the DNA triplex clamp can be readily tuned by adding unlabeled DNA strands of various length (8−13 bases, see inset) that allow formation of both Watson−Crick and Hoogsteen interactions of increasing stability. (b) Comparing the sensitivity of the tunable clamp switch (with stabilizer_10) and the 0GC stem-loop from 35 to 40 °C. The tunable clamp switch (green) and the 0GC stem-loop (black) emit 45% and 14% of their total fluorescence signal between the 35−40 °C interval, respectively. Inset: Normalized fluorescence output from 36.6 to 37.4 °C at 0.06 °C increments. The clamp switch (green) is found to be twice as precise than the 0GC stem-loop (black) within the 36−38 °C interval (±0.05 °C versus ±0.1 °C, respectively; see section "thermometer calibration" in Material and Methods). Experiments were conducted with 25 nM of switches and 100 nM of stabilizers in 50 mM HEPES with 300 mM NaCl and 10 mM $MgCl_2$ at pH 7.0 (clamp switch) and in 50 mM Na_2HPO_4 with 100 mM NaCl at pH 7.0 (0GC stem-loop).

precise temperature measurement down to 28 °C. However, these tri- and tetra-molecular thermoswitches also possess a higher fluorescent background at low temperature (>15%), which reduces their gain and the amplitude of the fluorescence signal available in their linear dynamic range. Of note, these tri- and tetra-meric switches could prove useful to build thermosensitive switches where multiple elements could be associated or dissociated in function of small temperature variations.[30]

Another important limitation of DNA stem-loop thermometers is that their melting transitions do not span a dynamic range larger than 12−15 °C (Figure 2a). This fixed dynamic range limits their capacity to measure temperature variations spanning more than 15 °C. In order to extend the linear dynamic range of DNA thermometers so that they respond to greater temperature variations, we set out to combine individual thermoswitches, each displaying varying melting temperatures (Figure 1d) (see for analogy refs 29 and 31). For example, by combining six stem-loops with increasing GC contents in the stem (from 0GC to 5GC), we are able to create a thermometer that displays a linear dynamic range spanning up to 48 °C (Figure 4a). Interestingly, such a mix of thermoswitches responds quite homogeneously to changes in sample condition (e.g., variation in salt concentration). For example, when the sensor is deployed at higher salt concentration this temperature sensor only shifts it dynamic range to higher temperature without affecting its range or linearity (Figure S5). Alternatively, by using our tunable stem-loop thermoswitch in combination with five unlabeled stabilizers of various lengths (18, 22, 24, 28, and 34 bases), we are also able to create a thermometer that displays a 46 °C wide dynamic range, similar

DOI: 10.1021/acs.nanolett.6b00156
Nano Lett. 2016, 16, 3976−3981

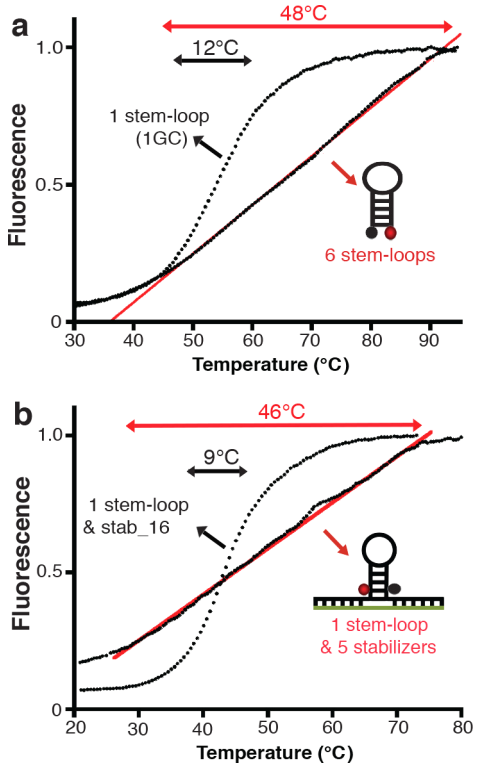

Figure 4. Extending the dynamic range of DNA nanothermometers by combining thermoswitches or by adding a mix of DNA stabilizers. (a) Extending the dynamic range of DNA nanothermometers by combining switches with different stabilities (0GC, 1GC, 2GC, 3GC, 4GC, 5GC). (b) Extending the dynamic range of a single DNA thermoswitch by adding a collection of DNA stabilizers of different lengths (Stab_18, stab_22, stab_24, stab_28, stab_34). Black circles represent data points and red lines represent linear fits. All experiments were conducted using 25 nM of fluorescent labeled stem-loops in 50 mM $NaPO_4$ with 100 mM NaCl at pH 7.0 (see Material and Methods for switches and stabilizers concentrations).

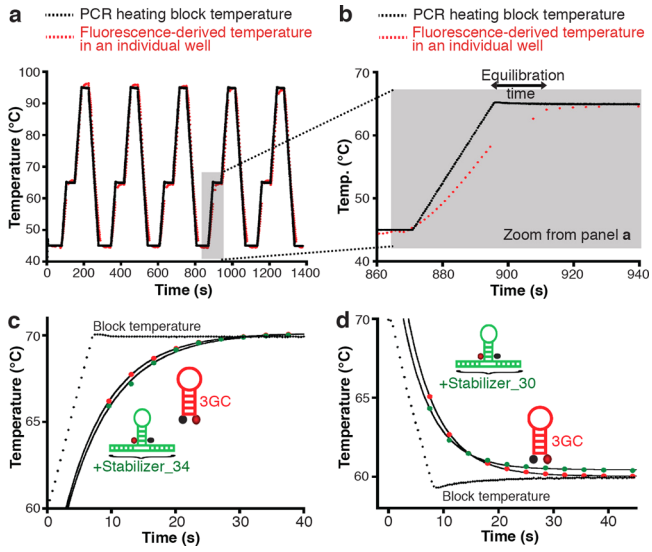

Figure 5. Real-time temperature monitoring in individual PCR wells using fluorescent DNA nanothermometers. (a) PCR cycles monitored using an "extended-range" thermometer that uses a combination of stem-loop thermoswitches (same stem-loop mix used than in Figure 2b). (b) Deviation between the PCR heating block temperature and the temperature measured inside individual wells using the fluorescent DNA nanothermometer (zoom from panel a). (c,d) Temperature equilibration rates inside a PCR well following rapid temperature jumps (1.35 °C/s) as monitored using two different DNA thermoswitches. In red, a 3GC stem-loop; in green, a stem-loop stabilized with a 34-nucleotide stabilizer (panel c) or a 30-nucleotide stabilizer (panel d). Temperature equilibration rates were found to be 0.14 and 0.13 s^{-1} while heating and 0.17 and 0.19 s^{-1} while cooling with the 3GC and stabilizer-tuned stem-loops thermometers, respectively. The small upward deviation (0.5 °C) observed for the stem-loop-stabilized thermometer in panel d is attributable to the limited linear dynamic range of this thermometer. Experiments were performed using 150 nM of mixed thermoswitches (panels a,b) in 50 mM Na_2HPO_4 and 300 mM NaCl at pH 7.0 or 50 nM of stem-loop (panels c,d) with 200 nM of stabilizer for the stabilizer-tuned stem-loop thermometer in 50 mM Na_2HPO_4 with 100 mM NaCl at pH 7.0.

to the extended thermometer made from a combination of 6 stem-loops (Figure 4b see for analogy ref 32). Notably, this "stabilizer" strategy significantly reduces the price of the extended thermometer from ~$1500 to roughly $300.

In order to illustrate the practicability and versatility of our programmable DNA thermometers, we employ them to monitor for the first time the temperature inside individual polymerase chain reactions (PCR) wells during several PCR cycles. To do so, we created a DNA thermometer that responds linearly within the temperature range of typical PCR experiments (i.e., from 45 to 93 °C) (Figure 4a). We first tested the reversibility of this fluorescent DNA thermometer by performing multiple, rapid temperature cycles over time (Figure 5a). This extended DNA thermometer (as well as other DNA thermometers, Figure S6) shows high reversibility over multiple cycles and displays high accuracy for temperature measurement when sufficient time is allowed for temperature equilibration. Interestingly, the thermometer also highlights a significant discrepancy between the block heater temperature and the temperature measured inside individual wells following rapid temperature jumps (Figure 5b). Becausee the stem-loop thermometer folds and unfolds faster than the millisecond time range (Figure S2), this observed equilibration time suggests that the sample inside each well may take several seconds before reaching the temperature indicated by the block heater (>10 s).

In order to precisely measure this equilibration time, we performed rapid 10 °C temperature jumps (i.e., 60 to 70 °C and 70 to 60 °C in 7.4 s) while monitoring sample temperature using two different thermometers with optimal sensitivity for this temperature range (a 3GC stem-loop and a stabilizer-tuned stem-loop) (Figure 5c,d). Temperature equilibration rates inside PCR wells were found to be 0.14 and 0.13 s^{-1} while heating and 0.17 and 0.19 s^{-1} while cooling when using the unimolecular 3GC and the stabilizer-tuned stem-loops thermometers, respectively. These results suggest that the sample temperature inside a PCR well only reaches the block heater temperature (±1 °C) 15 s after the block heater has reached it. Overall, this implies that sufficient equilibration time should be taken into consideration when using PCR instruments for quantitative purposes that require precise sample temperature measurements. For instance, DSF experiments,[33] which are employed to determine the strength of molecule–protein interactions, will overestimate the affinity if PCR melting transitions are performed too rapidly.

Here, we have engineered several DNA-based thermometers with programmable quantitative, linear dynamic ranges for optimal temperature monitoring at the nanoscale. More specifically, we have introduced various design strategies to tune "on-the-fly" the melting transition temperature and the cooperativity of

DOI: 10.1021/acs.nanolett.6b00156
Nano Lett. 2016, 16, 3976–3981

folding/unfolding transitions of these thermoswitches. Through structural modifications of the thermoswitch or via addition of inexpensive DNA stabilizers, we demonstrated that we can tune the transition midpoint from 30 to 85 °C. Through multimeric and triplex clamp switch architectures, we increased the thermoswitch sensitivity and created high gain thermoswitch that displays ∼3-fold higher signal gain then stem-loop thermometers. Through a combination of thermoswitches or via addition of a combination of inexpensive DNA stabilizers, we demonstrated that we can extend the linear, quantitative, dynamic range of the nanothermometer up to 50 °C. These programmable thermometers display two main advantages in comparison with previously published stem-loop based thermometers.[15−17] First, a single switch (e.g., the tunable stem-loop switch or the tunable triplex clamp switch) can now be reprogrammed and used for several applications including either precise temperature measurements within a small selected temperature window (e.g., see Figure 3b, Figure 5c-d) or for temperature measurement over wide-temperature ranges (see Figure 4b). Another novel feature of these tunable switches is that they may be reprogrammed "on-the-fly" within minutes in a specific experimental setup via the simple addition of inexpensive DNA strands.

In addition to their nanosize, fast response time (ms−s), high reversibility, and high programmability, the simple chemistry of DNA thermoswitches enables their adaption in multiple signaling formats. Using FRET fluorescent pairs and a ratiometric readout these switches appear particularly suitable for real-time temperature monitoring in the viscinity of enzymes,[34] in vivo[15,35,36] (see, for example, how structure-switching DNA pH meters enable one to monitor pH changes inside living cells)[37] or in nano- or microfluidic devices where local temperature at nanoscale may be of crucial importance.[38] These switches could also be attached to metal nanoparticules in order to accurately sense small temperature variations during laser-based nanosurgery[39] or magnetic hyperthermia treatments,[40] may help to optimize treatment. The DNA thermoswitches could also be adapted in an electrochemical format[41] and find applications in microfluidic devices such as point-of-care PCR instruments[42] which require multiple precise temperature settings despite external variations. Electrochemical DNA thermoswitches may also find applications in nanoelectronics to detect hotspots caused by defects in nanometric circuits.[1] Finally, these programmable DNA thermoswitches could be used to build thermosensitive structures that may find applications in the field of DNA nanomachines,[43] drug delivery systems[44] and macromolecular assemblies.[45] For example, thermoswitches could be incorporated into larger, drug carrying, DNA devices[46−48] in order to create thermally responsive systems that deliver their cargo via local temperature changes using either bodily temperature gradients or laser-induced heating.[49,50] Finally, these DNA thermosensitive structures could also inspire the design of thermally responsive RNA strands that could be genetically encoded in mRNA to reprogram gene expression so that it is induced at various specific temperatures.[51,52]

■ ASSOCIATED CONTENT

Supporting Information

The Supporting Information is available free of charge on the ACS Publications website at DOI: 10.1021/acs.nanolett.6b00156.

Material and Methods and supplementary figures. (PDF)

■ AUTHOR INFORMATION

Corresponding Author

*E-mail: a.vallee-belisle@umontreal.ca.

Author Contributions

The manuscript was written through contributions of all authors. All authors have given approval to the final version of the manuscript.

Funding

This work was supported by the National Sciences and Engineering Research Council of Canada through Grant 2014-06403 (NSERC) (A.V.B.). A.V.B. holds the Canada Research Chair in Bioengineering and Bionanotechnology, Tier II. D.G. is a CREATE NSERC fellow, and A.D. is a Fond de recherche Nature et technologies fellow (Québec, Canada).

Notes

The authors declare no competing financial interest.

■ ACKNOWLEDGMENTS

The authors acknowledge members of the Vallée-Bélisle laboratory, Dr. Andrea Idili and Liliana Pedro for helpful discussion on the manuscript.

■ REFERENCES

(1) Shakouri, B. A. *Proc. IEEE* **2006**, *94*, 1613.
(2) Nenna, G.; Flaminio, G.; Fasolino, T.; Minarini, C.; Miscioscia, R.; Palumbo, D.; Pellegrino, M. *Macromol. Symp.* **2007**, *247*, 326−332.
(3) Zhang, C.; Xing, D. *Nucleic Acids Res.* **2007**, *35* (13), 4223−37.
(4) Schroeder, A.; Heller, D. A.; Winslow, M. M.; Dahlman, J. E.; Pratt, G. W.; Langer, R.; Jacks, T.; Anderson, D. G. *Nat. Rev. Cancer* **2011**, *12*, 39−50.
(5) Yang, J. M.; Yang, H.; Lin, L. *ACS Nano* **2011**, *5* (6), 5067−71.
(6) Vetrone, F.; Naccache, R.; Zamarron, A.; Juarranz de la Fuente, A.; Sanz-Rodriguez, F.; Martinez Maestro, L.; Martin Rodriguez, E.; Jaque, D.; Garcia Sole, J.; Capobianco, J. A. *ACS Nano* **2010**, *4*, 3254−8.
(7) Fischer, L. H.; Harms, G. S.; Wolfbeis, O. S. *Angew. Chem., Int. Ed.* **2011**, *50*, 4546−51.
(8) Brites, C. D.; Lima, P. P.; Silva, N. J.; Millan, A.; Amaral, V. S.; Palacio, F.; Carlos, L. D. *Nanoscale* **2013**, *5*, 7572−80.
(9) Zhu, H.; Li, Y.; Qiu, R.; Shi, L.; Wu, W.; Zhou, S. *Biomaterials* **2012**, *33* (10), 3058−69.
(10) Fischer, L. H.; Harms, G. S.; Wolfbeis, O. S. *Angew. Chem., Int. Ed.* **2011**, *50*, 4546−4551.
(11) Kucsko, G.; Maurer, P. C.; Yao, N. Y.; Kubo, M.; Noh, H. J.; Lo, P. K.; Park, H.; Lukin, M. D. *Nature* **2013**, *500*, 54−8.
(12) Ye, F.; Wu, C.; Jin, Y.; Chan, Y. H.; Zhang, X.; Chiu, D. T. *J. Am. Chem. Soc.* **2011**, *133*, 8146−9.
(13) Okabe, K.; Inada, N.; Gota, C.; Harada, Y.; Funatsu, T.; Uchiyama, S. *Nat. Commun.* **2012**, *3*, 705.
(14) Donner, J. S.; Thompson, S. A.; Kreuzer, M. P.; Baffou, G.; Quidant, R. *Nano Lett.* **2012**, *12*, 2107−11.
(15) Ke, G.; Wang, C.; Ge, Y.; Zheng, N.; Zhu, Z.; Yang, C. J. *J. Am. Chem. Soc.* **2012**, *134*, 18908−11.
(16) Jonstrup, A. T.; Fredsoe, J.; Andersen, A. H. *Sensors* **2013**, *13* (5), 5937−5944.
(17) Ebrahimi, S.; Akhlaghi, Y.; Kompany-Zareh, M.; Rinnan, A. *ACS Nano* **2014**, *8*, 10372−82.
(18) Jaque, D.; Vetrone, F. *Nanoscale* **2012**, *4*, 4301−26.
(19) Brites, C. D.; Lima, P. P.; Silva, N. J.; Millan, A.; Amaral, V. S.; Palacio, F.; Carlos, L. D. *Nanoscale* **2012**, *4*, 4799−829.
(20) Vallee-Belisle, A.; Plaxco, K. W. *Curr. Opin. Struct. Biol.* **2010**, *20*, 518−26.
(21) Mura, S.; Nicolas, J.; Couvreur, P. *Nat. Mater.* **2013**, *12*, 991−1003.
(22) Kortmann, J.; Narberhaus, F. *Nat. Rev. Microbiol.* **2012**, *10*, 255−65.
(23) Tyagi, S.; Kramer, F. R. *Nat. Biotechnol.* **1996**, *14*, 303−8.

DOI: 10.1021/acs.nanolett.6b00156
Nano Lett. 2016, 16, 3976−3981

(24) Ricci, F.; Vallee-Belisle, A.; Porchetta, A.; Plaxco, K. W. *J. Am. Chem. Soc.* **2012**, *134*, 15177−80.
(25) Nayak, R. K.; Peersen, O. B.; Hall, K. B.; Van Orden, A. *J. Am. Chem. Soc.* **2012**, *134*, 2453−6.
(26) Doluca, O.; Withers, J. M.; Filichev, V. V. *Chem. Rev.* **2013**, *113* (5), 3044−83.
(27) Rachwal, P. A.; Fox, K. R. *Methods* **2007**, *43*, 291−301.
(28) Greschner, A. A.; Toader, V.; Sleiman, H. F. *J. Am. Chem. Soc.* **2012**, *134*, 14382−9.
(29) Idili, A.; Plaxco, K. W.; Vallée-Bélisle, A.; Ricci, F. *ACS Nano* **2013**, *7* (12), 10863−9.
(30) Bergueiro, J.; Calderon, M. *Macromol. Biosci.* **2015**, *15*, 183.
(31) Vallée-Bélisle, A.; Ricci, F.; Plaxco, K. W. *J. Am. Chem. Soc.* **2012**, *134*, 2876−2879.
(32) Porchetta, A.; Vallée-Bélisle, A.; Plaxco, K. W.; Ricci, F. *J. Am. Chem. Soc.* **2012**, *134*, 20601−20604.
(33) Niesen, F. H.; Berglund, H.; Vedadi, M. *Nat. Protoc.* **2007**, *2*, 2212−21.
(34) Riedel, C.; Gabizon, R.; Wilson, C. A.; Hamadani, K.; Tsekouras, K.; Marqusee, S.; Pressé, S.; Bustamante, C. *Nature* **2014**, *517*, 227−230.
(35) Kiyonaka, S.; Sakaguchi, R.; Hamachi, I.; Morii, T.; Yoshizaki, T.; Mori, Y. *Nat. Methods* **2015**, *12*, 801−802.
(36) Maestro, L. M.; Rodríguez, E. M.; Rodríguez, F. S.; la Cruz, M. I.-d.; Juarranz, A.; Naccache, R.; Vetrone, F.; Jaque, D.; Capobianco, J. A.; Solé, J. G. *Nano Lett.* **2010**, *10*, 5109−5115.
(37) Modi, S.; Swetha, M. G.; Goswami, D.; Gupta, G. D.; Mayor, S.; Krishnan, Y. *Nat. Nanotechnol.* **2009**, *4*, 325−330.
(38) Wu, J.; Kwok, T. Y.; Li, X.; Cao, W.; Wang, Y.; Huang, J.; Hong, Y.; Zhang, D.; Wen, W. *Sci. Rep.* **2013**, *3*, 3321.
(39) Boulais, E.; Lachaine, R.; Hatef, A.; Meunier, M. *J. Photochem. Photobiol., C* **2013**, *17*, 26−49.
(40) Martinez-Boubeta, C.; Simeonidis, K.; Makridis, A.; Angelakeris, M.; Iglesias, O.; Guardia, P.; Cabot, A.; Yedra, L.; Estrade, S.; Peiro, F.; Saghi, Z.; Midgley, P. A.; Conde-Leboran, I.; Serantes, D.; Baldomir, D. *Sci. Rep.* **2013**, *3*, 1652.
(41) Fan, C.; Plaxco, K. W.; Heeger, A. J. *Proc. Natl. Acad. Sci. U. S. A.* **2003**, *100*, 9134−9137.
(42) Fang, T. H.; Ramalingam, N.; Xian-Dui, D.; Ngin, T. S.; Xianting, Z.; Lai Kuan, A. T. L.; Peng Huat, E. Y. P.; Hai-Qing, G. *Biosens. Bioelectron.* **2009**, *24*, 2131−2136.
(43) Bath, J.; Turberfield, A. J. *Nat. Nanotechnol.* **2007**, *2*, 275−284.
(44) Schmaljohann, D. *Adv. Drug Delivery Rev.* **2006**, *58*, 1655−70.
(45) Zhuang, J.; Gordon, M. R.; Ventura, J.; Li, L.; Thayumanavan, S. *Chem. Soc. Rev.* **2013**, *42*, 7421−7435.
(46) Andersen, E. S.; Dong, M.; Nielsen, M. M.; Jahn, K.; Subramani, R.; Mamdouh, W.; Golas, M. M.; Sander, B.; Stark, H.; Oliveira, C. L.; Pedersen, J. S.; Birkedal, V.; Besenbacher, F.; Gothelf, K. V.; Kjems, J. *Nature* **2009**, *459*, 73−6.
(47) Edwardson, T. G.; Carneiro, K. M.; McLaughlin, C. K.; Serpell, C. J.; Sleiman, H. F. *Nat. Chem.* **2013**, *5*, 868−75.
(48) Douglas, S. M.; Bachelet, I.; Church, G. M. *Science* **2012**, *335*, 831−4.
(49) Schmaljohann, D. *Adv. Drug Delivery Rev.* **2006**, *58*, 1655−1670.
(50) Bergueiro, J.; Calderón, M. *Macromol. Biosci.* **2015**, *15*, 183−199.
(51) Neupert, J.; Karcher, D.; Bock, R. *Nucleic Acids Res.* **2008**, *36*, e124.
(52) Chang, A. L.; Wolf, J. J.; Smolke, C. D. *Curr. Opin. Biotechnol.* **2012**, *23*, 679−88.

DOI: 10.1021/acs.nanolett.6b00156
Nano Lett. 2016, 16, 3976−3981